International Journal of Engineering Science 49 (2011) 544–560

Contents lists available at ScienceDirect

International Journal of Engineering Science

journal homepage: www.elsevier.com/locate/ijengsci

Elastic moduli of solids containing spheroidal pores

E.C. David *, R.W. Zimmerman

Department of Earth Science and Engineering, Imperial College, London SW7 2AZ, United Kingdom

ARTICLE INFO

Article history:
Received 28 January 2011
Accepted 17 February 2011
Available online 21 March 2011

Keywords:
Porous materials
Elasticity
Differential effective medium
Pore aspect ratio
Poisson's ratio
Crack

ABSTRACT

We use asymptotic approximations for the elastic compliances (P, Q) of a spheroidal pore as input in the differential effective medium scheme to derive approximate analytical expressions for the effective moduli of an isotropic solid containing randomly oriented spheroids. The approximations are valid for crack-like pores having aspect ratios α as high as 0.3, needle-like pores having aspect ratios as low as 3, and nearly spherical pores ($0.7 < \alpha < 1.3$). Analytical solutions for the differential scheme have previously only been available for the limiting cases of infinitely thin-cracks ($\alpha = 0$) and spherical pores ($\alpha = 1$). The relatively simple approximations found between the limiting cases can account for more realistic pore shapes, and are valid for a wide range of porosities. The behaviour of the effective Poisson's ratio in the high concentration limit shows that v is bounded between the Poisson's ratio of the solid and a fixed point v_c that only depends on the aspect ratio of the pores. The asymptotic expressions for P and Q can also successfully be used as input in any other effective medium theory, such as the Mori–Tanaka or Kuster–Toksoz schemes. The relatively simple expressions found for the various effective medium schemes, as well as the bounds found for the effective Poisson's ratio, will be useful to simplify the process of inversion of elastic velocities in porous solids.

1. Introduction

Relating the effective elastic properties of porous solids to the pore structure is a classical problem in mechanics, with many applications in geophysics, materials and biomedical sciences, and many other fields. The effective properties of an isotropic solid containing randomly oriented voids depend on the elastic moduli of the minerals, on porosity but, also, on *pore shape*.

The assumption that the voids can be represented by *spheroids*, which can account for a wide variety of pore shapes and are characterized by their *aspect ratio*, α, offers the possibility of an analytical treatment. Indeed, exact expressions for the hydrostatic and shear compliances of spheroidal pores directly follow from Eshelby (1957). Unfortunately, Eshelby's ensuing expressions for the effective moduli of a material containing these pores are only valid at very small inclusion concentrations. Extending the small-concentration results to higher concentrations has proven to be a difficult task: indeed, the complexity of the interactions of stress and strain fields between nearby pores renders an exact treatment impossible. Among the various approximate schemes proposed to do this, commonly known as effective medium theories, the *differential effective medium* theory (McLaughlin, 1977; Norris, 1985; Salganik, 1973; Zimmerman, 1984) calculates the effective elastic moduli by considering that inclusions are introduced into the body in small amounts, with the effective moduli re-calculated at each step; this leads to a pair of differential equations for the effective bulk and shear moduli. The predictions of the differential scheme always lie within the rigorous bounds derived by Hashin and Shtrikman (1961).

* Corresponding author. Tel.: +44 (0) 20 759 47135; fax: +44 (0) 20 759 47444.
E-mail addresses: emmanuel.david08@imperial.ac.uk (E.C. David), r.w.zimmerman@imperial.ac.uk (R.W. Zimmerman).

0020-7225/$ - see front matter
doi:10.1016/j.ijengsci.2011.02.001

Evidence has been accruing to show that the differential scheme is quite accurate even at high inclusions concentrations. This evidence comes from comparisons with numerical simulations (see, among others, (Saenger, Kruger, & Shapiro, 2004, 2006; Shen & Li, 2004)); and with a few sets of experimental data obtained on synthetic materials (Carvalho & Labuz, 1996; Zimmerman, 1991a).

However, analytical solutions for the differential scheme have only been given so far in the limiting cases of infinitely thin cracks ($\alpha \to 0$) and spherical pores ($\alpha = 1$), respectively by Zimmerman (1991a, 1991b), Berryman, Pride, and Wang (2002) examined the case of infinitely for infinitely long needles ($\alpha \to \infty$), but they did not give explicit solutions. Apart from the limiting cases, exact solutions can only be obtained by numerical integration. This is why most works have used only the simple solutions available in the limiting cases. Nevertheless, cracks are never infinitely thin, pores are never perfectly spherical, and cylindrical pores are never infinitely long. Hence, it would be useful to have approximate analytical solutions for the differential scheme, that are valid for more realistic pore geometries in *between* the limiting cases. The asymptotic expressions for P and Q recently presented by David and Zimmerman (2011) for crack-like, nearly spherical and needle-like pores, cover accurately a wide range of aspect ratios. They can be used as input in the differential scheme, as well as in any other effective medium theory. The first goal of our study is then to present asymptotic solutions for the differential scheme (Section 3). The results will be then compared to those obtained if we use the expressions for P and Q as input in the "effective-field" method of Mori and Tanaka (1973) and the "wave-scattering" theory of Kuster and Toksoz (1974), in Section 4.

The effective Poisson's ratio, v, is directly related to the ratio of compressional to shear wave velocities. It has long been used (in earth sciences, notably) because of its sensitivity to the microstructure (Wilkens, Simmons, & Caruso, 1984). For dry porous solids, v is only a function of the porosity, the pore aspect ratio and the Poisson's ratio of the solid. We could use measurements of v as a diagnostic tool for studying the pore structure. The last aim of our study is to then look at the behaviour of Poisson's ratio in the high-concentration limit, using the exact results for the differential scheme. Previously, the special case of spherical pores have been examined in detail by Zimmerman (1994). For a general spheroid, useful discussions have been given in Berryman et al. (2002) for the differential scheme, and Dunn and Ledbetter (1995) for the Mori–Tanaka scheme. Fixed-points and possible bounds for the effective Poisson's ratio will be discussed in Section 5.

2. General equations for the differential effective medium (DEM) theory

Consider an isotropic solid of bulk and shear moduli (K_0, G_0), respectively, comprising spheroidal pores having the same aspect ratio α, acting here as a *fixed parameter*. If the inclusions have random orientations, the overall effective medium can be assumed to be isotropic. We can then use the expressions obtained by David and Zimmerman (2011) for the normalized pore compressibility, P, and pore shear compliance, Q to calculate the effective bulk and shear moduli (K, G). According to the *differential effective medium* theory, the effective moduli are described by a pair of coupled differential equations (LeRavalec & Gueguen, 1996):

$$(1-\phi)\frac{1}{K}\frac{dK}{d\phi} = -P(v), \tag{1}$$

$$(1-\phi)\frac{1}{G}\frac{dG}{d\phi} = -Q(v) \tag{2}$$

with the initial conditions

$$K(\phi = 0) = K_0, \tag{3}$$

$$G(\phi = 0) = G_0, \tag{4}$$

where ϕ is the porosity, and v is the effective Poisson's ratio, given by:

$$v = \frac{3K - 2G}{6K + 2G}. \tag{5}$$

The term $(1 - \phi)$ on the left-hand side of Eqs. (1) and (2) accounts for the fact that each new pore introduced in the body may replace either the solid phase or the porous phase, with probabilities ϕ and $(1 - \phi)$, respectively (McLaughlin, 1977; Norris, 1985). Because P and Q both depend on the "current" Poisson's ratio, v, which in turn is a function of the effective moduli K and G (Eq. (5)), the two differential Eqs. (1) and (2) are *coupled*. However, they can be converted to a set of uncoupled differential equations by simple manipulations. First, form a differential equation for the Poisson's ratio, v, by differentiating Eq. (5):

$$\frac{dv}{d\phi} = \frac{18KG}{(6K+2G)^2}\left(\frac{1}{K}\frac{dK}{d\phi} - \frac{1}{G}\frac{dG}{d\phi}\right) \tag{6}$$

and then by combining Eq. (6) with (1) and (2):

$$(1-\phi)\frac{dv}{d\phi} \equiv F_v(v) = \frac{(1+v)(1-2v)}{3}[Q(v) - P(v)]. \tag{7}$$

Now, divide one of the two ODEs, (1) or (2), by (7) to obtain another uncoupled differential equation in the "phase" space, (K, v), or (G, v). If we decide to work in the (K, v) space, we obtain, by dividing Eqs. (1) and (7):

$$\frac{1}{K}\frac{\mathrm{d}K}{\mathrm{d}v} \equiv F_K(v) = \frac{3}{(1+v)(1-2v)}\left[\frac{P(v)}{P(v)-Q(v)}\right]. \tag{8}$$

Hence, using the initial condition $v(\phi = 1) = v_0$, where v_0 therefore denotes the solid's Poisson's ratio, the general solutions of the system of ODEs can be written as follows:

$$-\ln(1-\phi) = \int_{v_0}^{v} \frac{1}{F_v(v)}\mathrm{d}v,, \tag{9}$$

$$\ln\left(\frac{K}{K_0}\right) = \int_{v_0}^{v} F_K(v)\ \mathrm{d}v. \tag{10}$$

In the general case of a spheroid of arbitrary aspect ratio, P and Q are cumbersome functions of α and v (David & Zimmerman, 2011). In the next section, we derive new approximate expressions for the differential scheme between the limiting cases. For crack-like, needle-like and nearly spherical pores, we use the asymptotic expressions for P and Q recently presented by David and Zimmerman (2011) as input in the set of Eqs. (7) and (8).

3. Asymptotic solutions for the DEM in the limiting cases

3.1. Crack-like pores

The volume occupied by cracks is small, but their compliances are quite large, since they are, to first order, inversely proportional to the aspect ratio (see Eqs. (13) and (14) below). Hence, the relevant microstructural parameter that influences the effective elastic properties of cracked solids is not the porosity, but rather a parameter proportional to the volume of the distorted strain field around a crack (Henyey & Pomphrey, 1982). We recall the following definition of the crack density Γ (Walsh, 1965):

$$\Gamma = \frac{N < a^3 >}{V}, \tag{11}$$

where N is the number of circular cracks (of radius a) in a representative elementary volume V, and the angle brackets symbolize an average. The crack density is then related to the total porosity ϕ by

$$\phi = \frac{4}{3}\pi\alpha\Gamma. \tag{12}$$

3.1.1. Thin cracks

The bulk and shear compliance of an *infinitely thin crack* ($\alpha \to 0$) are both inversely proportional to α:

$$P = \frac{4(1-v^2)}{3\pi\alpha(1-2v)}, \tag{13}$$

$$Q = \frac{8(1-v)(5-v)}{15\pi\alpha(2-v)}. \tag{14}$$

Subsituting the expressions for P and Q (13), (14) in the set of differential Eqs. (7), (8), and changing variables to work with the crack density Γ instead of the porosity (Eq. (12)), we obtain, in the limit $\alpha \to 0$, a simple set of equations:

$$\frac{\mathrm{d}v}{\mathrm{d}\Gamma} = \frac{-16v(1-v^2)(3-v)}{15(2-v)}, \tag{15}$$

$$\frac{1}{K}\frac{\mathrm{d}K}{\mathrm{d}v} = \frac{5(2-v)}{3v(1-2v)(3-v)}, \tag{16}$$

which, using partial fractions, immediately leads to an implicit solution as found by Zimmerman (1985):

$$\frac{128\Gamma}{5} = \ln\left(\frac{3-v}{3-v_0}\right) + 6\ln\left(\frac{1-v}{1-v_0}\right) + 9\ln\left(\frac{1+v}{1+v_0}\right) - 16\ln\left(\frac{v}{v_0}\right), \tag{17}$$

$$\frac{K}{K_0} = \left(\frac{v}{v_0}\right)^{\frac{10}{9}}\left(\frac{3-v}{3-v_0}\right)^{\frac{-1}{9}}\left(\frac{1-2v}{1-2v_0}\right)^{-1}. \tag{18}$$

Considerably simpler solutions can be found retaining only the leading terms, i.e., the terms in Eqs. (17) and (18) that are unbounded throughout the physically meaningful range $0 < v < 0.5$ (Zimmerman, 1991a):

$$\Gamma = \frac{5}{8}\ln\left(\frac{\nu}{\nu_0}\right), \tag{19}$$

$$\frac{K}{K_0} = \left(\frac{\nu}{\nu_0}\right)^{\frac{10}{9}}\left(\frac{1-2\nu}{1-2\nu_0}\right)^{-1}, \tag{20}$$

thus recovering the approximate solutions previously found by Bruner (1976). Having such simple solutions has the advantage of giving (ν, K) as explicit functions of Γ:

$$\frac{\nu}{\nu_0} = \mathrm{e}^{-8\Gamma/5}, \tag{21}$$

$$\frac{K}{K_0} = \frac{(1-2\nu_0)\ \mathrm{e}^{-16\Gamma/9}}{1-2\nu_0\ \mathrm{e}^{-8\Gamma/5}}. \tag{22}$$

The accuracy of the expressions (21), (22) depend slightly on the value of the initial Poisson's ratio, ν_0; however, the error remains less than 2%, even at very high crack densities.

3.1.2. Crack-like oblate spheroids

The solutions above (Eqs. (21) and (22)) are well established in the literature (Benveniste, 1987; Bruner, 1976; Zimmerman, 1985, 1991a). However, they are only valid when the cracks have very small aspect ratios: the assumption that P and Q are assumed to be inversely proportional to α is, strictly speaking, only valid when α does not exceed 0.01. David and Zimmerman (2011) have recently found simple expressions for the pore compliances that are accurate for values of α as high as 0.3, taking only two more terms in the series expansions for both P and Q:

$$P \sim \frac{P_{-1}}{\alpha} + P_0 + P_1\alpha, \tag{23}$$

$$Q \sim \frac{Q_{-1}}{\alpha} + Q_0 + Q_1\alpha, \tag{24}$$

where (P_{-1}, Q_{-1}) follow from Eqs. (13) and (14):

$$P_{-1} = \frac{4(1-\nu^2)}{3\pi(1-2\nu)}, \tag{25}$$

$$Q_{-1} = \frac{8(1-\nu)(5-\nu)}{15\pi(2-\nu)} \tag{26}$$

and with

$$P_0 = \frac{1}{6}(1-\nu)(1-2\nu), \tag{27}$$

$$P_1 = \frac{(1+\nu)(1-\nu)}{12(1-2\nu)}\left[\pi(1-2\nu)^2 + \frac{8(7-8\nu)}{\pi}\right], \tag{28}$$

$$Q_0 = \frac{2}{15}\left[(5-2\nu^2) + \frac{48(1-\nu)(3-\nu)}{\pi^2(2-\nu)^2}\right] \tag{29}$$

$$Q_1 = \frac{\pi}{120}\left[\frac{37-8\nu(3+4\nu-2\nu^3)}{1-\nu}\right] + \frac{4(1-\nu)}{15\pi(2-\nu)^2}\left[-8(7+\nu^3) + 3\nu(9\nu-1) + \frac{96(3-\nu)^2}{\pi^2(2-\nu)}\right]. \tag{30}$$

Using the asymptotic expressions for P and Q above as input in the differential scheme, approximate solutions for the differential scheme can be found. This derivation involves various assumptions and calculation steps, which are detailed here and will be applied subsequently for the cases of needle-like (Section 3.2) and nearly spherical pores (Section 3.3). First of all, if we insert the asymptotic expresions for P and Q (Eqs. (23) and (24)) in the two uncoupled differential equations for $\phi(\nu)$ and $K(\nu)$, (7) and (8), the pair of differential equations becomes:

$$\left(1 - \frac{4}{3}\pi\alpha\Gamma\right)^{-1}\frac{\mathrm{d}\Gamma}{\mathrm{d}\nu} = \left[\frac{9}{4\pi(1+\nu)(1-2\nu)}\right]\left[\frac{1}{(Q_{-1}-P_{-1}) + (Q_0-P_0)\alpha + (Q_1-P_1)\alpha^2}\right], \tag{31}$$

$$\frac{1}{K}\frac{\mathrm{d}K}{\mathrm{d}\nu} = \left[\frac{3}{(1+\nu)(1-2\nu)}\right]\left[\frac{P_{-1} + P_0\alpha + P_1\alpha^2}{(P_{-1}-Q_{-1}) + (P_0-Q_0)\alpha + (P_1-Q_1)\alpha^2}\right]. \tag{32}$$

Note that in the case of crack-like pores, we have changed variables from ϕ to Γ in the first Eq. (7), using (12). Because of the relative complexity of the sum of terms in the denominator, an analytical integration of Eqs. (31) and (32) is, unfortunately, still not possible. A further simplification can be made by noting that since α is small, we can expand the denominators in Taylor series. Retaining only the terms up to α^2, we arrive at equations of the form

$$\left(1-\frac{4}{3}\pi\alpha\Gamma\right)^{-1}\frac{d\Gamma}{d\nu}=\left[\frac{9}{4\pi(1+\nu)(1-2\nu)}\right]\times\left[\frac{1}{Q_{-1}-P_{-1}}\right]\left\{1-\left(\frac{Q_0-P_0}{Q_{-1}-P_{-1}}\right)\alpha+\left[-\frac{Q_1-P_1}{Q_{-1}-P_{-1}}+\frac{(Q_0-P_0)^2}{(Q_{-1}-P_{-1})^2}\right]\alpha^2\right\}, \tag{33}$$

$$\frac{1}{K}\frac{dK}{d\nu}=\left[\frac{3}{(1+\nu)(1-2\nu)}\right]\left[\frac{P_{-1}}{P_{-1}-Q_{-1}}\right]\times\left\{1+\left[-\frac{P_0-Q_0}{P_{-1}-Q_{-1}}+\frac{P_0}{P_{-1}}\right]\alpha+\left[\frac{P_1}{P_{-1}}-\frac{P_0(P_0-Q_0)}{P_{-1}(P_{-1}-Q_{-1})}-\frac{P_1-Q_1}{P_{-1}-Q_{-1}}+\frac{(P_0-Q_0)^2}{(P_{-1}-Q_{-1})^2}\right]\alpha^2\right\}. \tag{34}$$

Eqs. (33) and (34) can be integrated using partial fractions. The solution is a cumbersome sum of terms involving logarithms and rational functions of Poisson's ratio. However, as previously done for thin cracks (Eqs. (19) and (20)), the solutions can be considerably simplified, without losing accuracy, by retaining only the unbounded terms,. This yields final expressions of the form

$$\left(\frac{-3}{4\pi\alpha}\right)\ln\left(1-\frac{4}{3}\pi\alpha\Gamma\right)=-\frac{5}{8}\ln\left(\frac{\nu}{\nu_0}\right)+\alpha\left[c_1\ln\left(\frac{\nu}{\nu_0}\right)+c_2\left(\frac{1}{\nu}-\frac{1}{\nu_0}\right)\right]+\alpha^2\left[c_3\ln\left(\frac{\nu}{\nu_0}\right)+c_4\left(\frac{1}{\nu}-\frac{1}{\nu_0}\right)+c_5\left(\frac{1}{\nu^2}-\frac{1}{\nu_0^2}\right)\right], \tag{35}$$

$$\ln\left(\frac{K}{K_0}\right)=\left[\frac{10}{9}\ln\left(\frac{\nu}{\nu_0}\right)-\ln\left(\frac{1-2\nu}{1-2\nu_0}\right)\right]+\alpha\left[C_1\ln\left(\frac{\nu}{\nu_0}\right)+C_2\left(\frac{1}{\nu}-\frac{1}{\nu_0}\right)\right]+\alpha^2\left[C_3\ln\left(\frac{\nu}{\nu_0}\right)+C_4\left(\frac{1}{\nu}-\frac{1}{\nu_0}\right)+C_5\left(\frac{1}{\nu^2}-\frac{1}{\nu_0^2}\right)\right], \tag{36}$$

where

$$c_1=\frac{25}{864}\left(\frac{48}{\pi}+\pi\right)\approx 0.533, \tag{37}$$

$$c_2=\frac{5}{288}\left(\frac{48}{\pi}+5\pi\right)\approx 0.538, \tag{38}$$

$$c_3=\frac{5}{81}\left(\frac{82}{\pi^2}-\frac{163}{16}+\frac{1753}{1536}\pi^2\right)\approx 0.579, \tag{39}$$

$$c_4=\frac{5}{27}\left(\frac{8}{\pi^2}-\frac{61}{6}+\frac{137}{768}\pi^2\right)\approx -1.407, \tag{40}$$

$$c_5=\frac{5}{9}\left(\frac{1}{\pi}+\frac{5\pi}{48}\right)^2\approx 0.232 \tag{41}$$

and

$$C_1=\frac{5}{972}\left(\frac{96}{\pi}+77\pi\right)\approx 1.402, \tag{42}$$

$$C_2=-\frac{5}{162}\left(\frac{48}{\pi}+5\pi\right)\approx -0.956, \tag{43}$$

$$C_3=\frac{5}{243}\left(\frac{863}{288}\pi^2-64+\frac{320}{3\pi^2}\right)\approx -0.486, \tag{44}$$

$$C_4=\frac{5}{243}\left(-\frac{47\pi^2}{8}+\frac{341}{3}-\frac{320}{\pi^2}\right)\approx 0.479, \tag{45}$$

$$C_5=-\frac{5}{11664}\left(\frac{48}{\pi}+5\pi\right)^2\approx -0.412. \tag{46}$$

Taking the limit $\alpha \to 0$ in both sides of Eqs. (35) and (36), we recover Bruner's solution (Bruner, 1976) for thin cracks (19), (20), as expected.

For different values of α, and assuming that the solid's Poisson's ratio ν_0 is equal to 0.25, the predictions of the asymptotic expressions (35) and (36) for the Poisson's ratio and normalized bulk modulus are compared to the exact solutions for the differential scheme in Figs. 1 and 2, respectively. We also show Bruner's solution for infinitely thin cracks, which is recovered by taking $\alpha = 0$ in the Eqs. (35) and (36). For infinitely thin cracks, the difference between the Bruner's solution, and the exact solution (Eqs. (17) and (18)), would not be visible on the figures.

The approximate expressions (35) and (36) are, as expected, more accurate for smaller values of the pore aspect ratio, α, and smaller values of the crack density, Γ. For a solid having a Poisson's ratio $\nu = 0.25$, for $\alpha = 0.01$ the error on both K and ν is negligible. Furthermore, it is interesting to note that, even for an aspect ratio as low as 0.01, assuming that the cracks are infinitely thin would introduce a small but significant error on the estimates of the elastic moduli, particularly for ν (Fig. 1). For $\alpha = 0.1$, the error in the predictions of both moduli is still less than 3% for $\Gamma = 0.70$ ($\sim\phi = 30\%$). For $\alpha = 0.3$, the error on K and ν remains less than 3% only up to $\Gamma = 0.12$ ($\sim\phi = 15$ %) and $\Gamma = 0.24$ ($\sim\phi = 30$ %), respectively.

The accuracy of the asymptotic solutions also depends strongly on ν_0, the solid's Poisson's ratio, as shown in Fig. 3, where we show the behaviour of ν for different initial values of ν_0, and for $\alpha = 0.3$. At high crack densities, the exact solutions drive the Poisson's ratio to a critical value ν_c, which independent of ν_0, and which, for $\alpha = 0.3$, is approximately given by $\nu_c = 0.16$. On the other hand, the infinitely-thin-crack limit predicts that ν goes to zero as the crack density increases (Fig. 3).

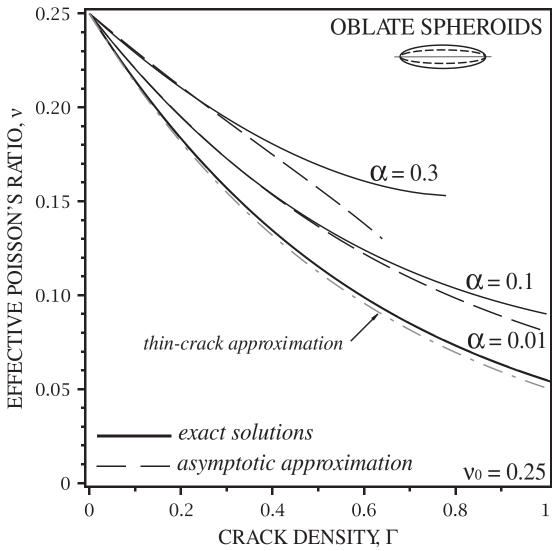

Fig. 1. Effective Poisson's ratio of a solid containing spheroidal pores, for three values of the spheroid aspect ratio ($\alpha = 0.01$; $\alpha = 0.1$; $\alpha = 0.3$), according to the asymptotic solution (Eq. (35)) (dashed line), and the exact solution (full line), which is obtained by numerical integration of Eq. (9), using the exact solutions for P and Q as given David and Zimmerman (2011). The Poisson's ratio of the solid is $\nu_0 = 0.25$.

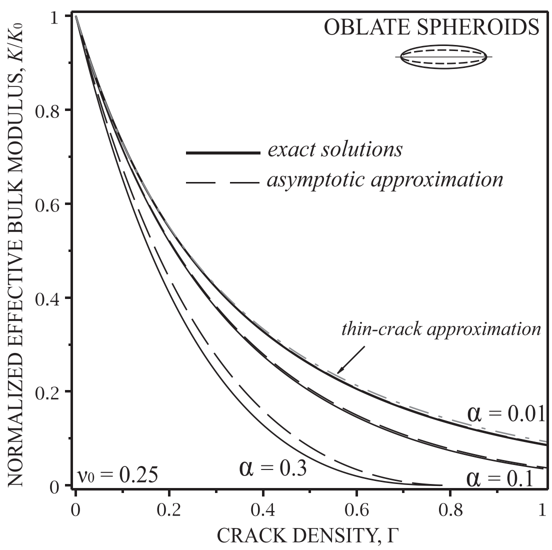

Fig. 2. Normalized effective bulk modulus of a solid containing spheroidal pores, for three values of the spheroid aspect ratio ($\alpha = 0.01$; $\alpha = 0.1$; $\alpha = 0.3$), according to the asymptotic solution (combining Eqs. (35) and (36)), and the exact solution, which is obtained by numerical integration of Eqs. (9) and (10), using the exact solutions for P and Q as given in David and Zimmerman (2011). The Poisson's ratio of the solid is $\nu_0 = 0.25$.

3.2. Needle-like pores

3.2.1. Infinitely long needles

At the other end of the aspect ratio spectrum, for infinitely long needles ($\alpha \to \infty$), P and Q take on the following finite values:

$$P \to \frac{5-4v}{3(1-2v)}, \tag{47}$$

$$Q \to \frac{8(5-3v)}{15}. \tag{48}$$

In this case, the two uncoupled differential Eqs. (7) and (8) then become:

$$(1-\phi)\frac{dv}{d\phi} = \frac{1}{15}(16v^2 - 28v + 5)(1+v), \tag{49}$$

$$\frac{1}{K}\frac{dK}{dv} = -\frac{5(5-4v)}{(16v^2-28v+5)(1-2v)(1+v)}, \tag{50}$$

from which an implicit solution can be found, again using partial fractions:

$$\frac{98}{15}\ln(1-\phi) = -2\ln\left(\frac{1+v}{1+v_0}\right) + \left(1-\frac{15}{\sqrt{29}}\right)\ln\left(\frac{7+\sqrt{29}-8v}{7+\sqrt{29}-8v_0}\right) + \left(1+\frac{15}{\sqrt{29}}\right)\ln\left(\frac{7-\sqrt{29}-8v}{7-\sqrt{29}-8v_0}\right), \tag{51}$$

$$\ln\left(\frac{K}{K_0}\right) = -\ln\left(\frac{1-2v}{1-2v_0}\right) - \frac{15}{49}\ln\left(\frac{1+v}{1+v_0}\right) + \frac{2}{49}\left(16+\frac{93}{\sqrt{29}}\right)\ln\left(\frac{7-\sqrt{29}-8v}{7-\sqrt{29}-8v_0}\right) + \frac{2}{49}\left(16-\frac{93}{\sqrt{29}}\right)\ln\left(\frac{7+\sqrt{29}-8v}{7+\sqrt{29}-8v_0}\right). \tag{52}$$

Although these solutions are exact, they are still cumbersome. As previously done for the case of thin cracks (Section 3.1), we can considerably simplify the solutions by retaining only those terms on the right-hand side that remain unbounded as $\phi \to 1$, incurring an error that will be less than 1%, almost regardless of the value of v_0. This yields an approximate solution of the form

$$(1-\phi) = \left(\frac{\lambda - v}{\lambda - v_0}\right)^{n_1}, \tag{53}$$

$$\frac{K}{K_0} = \left(\frac{1-2v}{1-2v_0}\right)^{-1}\left(\frac{\lambda - v}{\lambda - v_0}\right)^{N_1}, \tag{54}$$

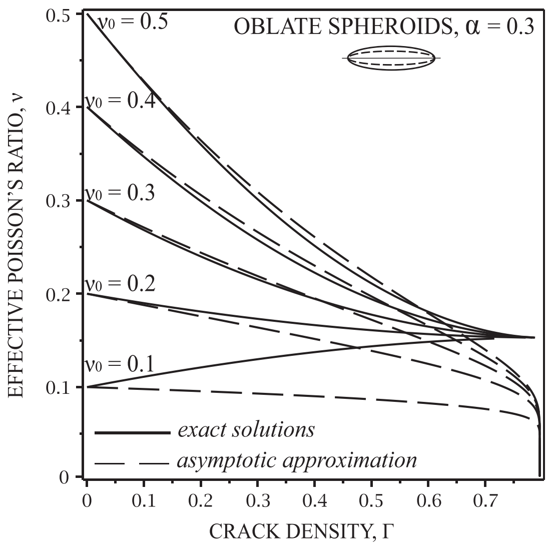

Fig. 3. Effective Poisson's ratio of a solid containing spheroidal pores, for five different values of the solid's Poisson's ratio ($v_0 = 0.1$; $v_0 = 0.2$; $v_0 = 0.3$; $v_0 = 0.4$; $v_0 = 0.5$), according to the asymptotic solution (35) (dashed line), and the exact solution (full line), for the differential scheme. The pores have an aspect ratio $\alpha = 0.3$.

where

$$\lambda = \frac{7-\sqrt{29}}{8} \approx 0.202, \tag{55}$$

$$n_1 = \frac{15}{98}\left(1+\frac{15}{\sqrt{29}}\right) \approx 0.579, \tag{56}$$

$$N_1 = \frac{2}{49}\left(16+\frac{93}{\sqrt{29}}\right) \approx 1.358, \tag{57}$$

which therefore gives the effective constants as explicit functions of the porosity:

$$v = \lambda - (\lambda - v_0)(1-\phi)^{1/n_1}, \tag{58}$$

$$\frac{K}{K_0} = \left\{\frac{1-2\left[\lambda-(\lambda-v_0)(1-\phi)^{1/n_1}\right]}{1-2v_0}\right\}^{-1}(1-\phi)^{N_1/n_1}. \tag{59}$$

3.2.2. Needle-like prolate spheroids

David and Zimmerman (2011) recently presented asymptotic expressions for the compliances of needle-like pores having finite aspect ratios, that are accurate for values of α as low as 2 for the shear compressibility P, and as low as 3 for the shear compliance Q, with less than 0.5% error:

$$P \sim \frac{5-4v}{3(1-2v)} + \frac{(1+v)\{4(1-v)[1-\ln(2\alpha)]-1\}}{6(1-2v)(1-v)\alpha^2}, \tag{60}$$

$$Q \sim \frac{8(5-3v)}{15} + \frac{4}{15(1-v)\alpha^2}\left\{3v(2-v)-1+\left[13-43v+12v^2(5-2v)\right][1-\ln(2\alpha)]\right\}. \tag{61}$$

If these approximate expressions for P and Q are used as input in the set of differential Eqs. (7) and (8), an analytical integration is still not possible. However, noting that in this case the term $1/\alpha^2$ is a small parameter, we can proceed as we did for crack-like pores (Section 3.1), again retaining only the leading terms. Extensive calculations yield implicit solutions for the effective moduli in the form:

$$\ln(1-\phi) = n_1 \ln\left(\frac{\lambda-v}{\lambda-v_0}\right) + \frac{1}{\alpha^2}\left\{[n_2+n_3\ln(2\alpha)]\times\ln\left(\frac{\lambda-v}{\lambda-v_0}\right) + [n_4+n_5\ln(2\alpha)]\left(\frac{1}{\lambda-v}-\frac{1}{\lambda-v_0}\right)\right\}, \tag{62}$$

$$\begin{aligned}\ln\left(\frac{K}{K_0}\right) &= -\ln\left(\frac{1-2v}{1-2v_0}\right) + N_1\ln\left(\frac{\lambda-v}{\lambda-v_0}\right) \\ &\quad + \frac{1}{\alpha^2}\left\{[N_2+N_3\ln(2\alpha)]\ln\left(\frac{\lambda-v}{\lambda-v_0}\right) + [N_4+N_5\ln(2\alpha)]\left(\frac{1}{\lambda-v}-\frac{1}{\lambda-v_0}\right)\right\}.\end{aligned} \tag{63}$$

where

$$n_2 = -\frac{14415}{9604}\left(1-\frac{72161}{27869\sqrt{29}}\right) \approx -0.779, \tag{64}$$

$$n_3 = \frac{510}{343}\left(1-\frac{103}{58\sqrt{29}}\right) \approx 0.997, \tag{65}$$

$$n_4 = \frac{135}{2842}\left(1+\frac{2}{9}\sqrt{29}\right) \approx 0.104, \tag{66}$$

$$n_5 = -\frac{15}{812}\left(1+\frac{\sqrt{29}}{2}\right) \approx -0.068, \tag{67}$$

$$N_2 = -\frac{970}{2401}\left(1+\frac{11276}{2813\sqrt{29}}\right) \approx -0.705, \tag{68}$$

$$N_3 = \frac{230}{343}\left(1+\frac{5387}{1334\sqrt{29}}\right) \approx 1.173, \tag{69}$$

$$N_4 = \frac{345}{2842}\left(1+\frac{13}{69}\sqrt{29}\right) \approx 0.245, \tag{70}$$

$$N_5 = -\frac{25}{1624}(5+\sqrt{29}) \approx -0.160. \tag{71}$$

In the asymptotic expressions (62) and (63), taking the limit as $\alpha \to \infty$ recovers the expressions found previously for infinitely long needles (Eqs. (53) and (54)).

These approximate asymptotic solutions are accurate for prolate spheroids having aspect ratios as low as 3, as seen in Figs. 4 and 5.

3.3. Nearly spherical pores

3.3.1. Spheres

For perfectly spherical pores ($\alpha = 1$), the expressions for P and Q are:

$$P = \frac{3(1-\nu)}{2(1-2\nu)}, \tag{72}$$

$$Q = \frac{15(1-\nu)}{7-5\nu}. \tag{73}$$

The set of differential Eqs. (7) and (8) becomes, in this case,

$$(1-\phi)\frac{d\nu}{d\phi} = \frac{3}{2}\frac{(1-\nu^2)(1-5\nu)}{7-5\nu}, \tag{74}$$

$$\frac{1}{K}\frac{dK}{d\nu} = \frac{-(7-5\nu)}{(1-5\nu)(1-2\nu)(1+\nu)}, \tag{75}$$

which, using partial fractions, is easily integrated to yield

$$(1-\phi) = \left(\frac{1-\nu}{1-\nu_0}\right)^{-\frac{1}{6}}\left(\frac{1-5\nu}{1-5\nu_0}\right)^{\frac{5}{6}}\left(\frac{1+\nu}{1+\nu_0}\right)^{-\frac{2}{3}}, \tag{76}$$

$$\frac{K}{K_0} = \left(\frac{1-5\nu}{1-5\nu_0}\right)^{\frac{5}{3}}\left(\frac{1-2\nu}{1-2\nu_0}\right)^{-1}\left(\frac{1+\nu}{1+\nu_0}\right)^{-\frac{2}{3}}. \tag{77}$$

recovering the solutions found by Zimmerman (1985). Contrary to the previous cases of cracks and needles, the solutions for spherical pores (76), (77) cannot be well approximated by retaining only the leading terms (i.e., the terms involving $1-5\nu$). Indeed, this would introduce an error of more than 3%. Note, however, that Zimmerman (1991b) has shown that if the system of differential equations are decoupled and integrated in terms of the variables (K,G) instead of (K,ν), the resulting expressions are simpler, eliminating the need to discard lower-order terms. This approach will not be pursued further in the present paper, however.

3.3.2. Slightly deformed spheres

A perfectly spherical pore possesses the minimum possible values of the pore compliances (David & Zimmerman, 2011). For nearly spherical pores, David and Zimmerman (2011) recently derived asymptotic expressions for P and Q that are valid for $0.7 < \alpha < 1.3$ with less than 0.5% error, by considering terms that are quadratic and cubic in $(1-\alpha)$:

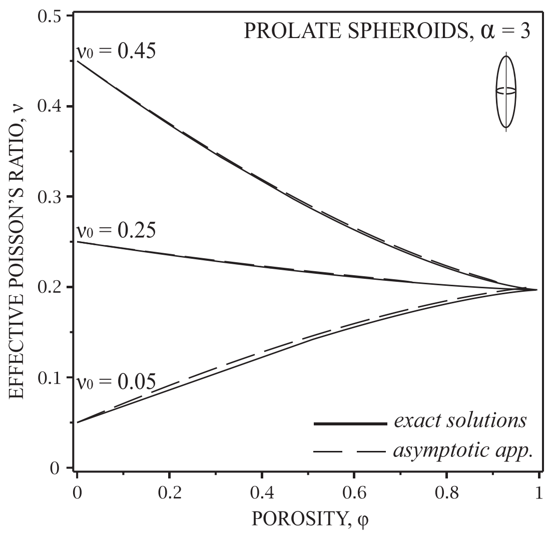

Fig. 4. Effective Poisson's ratio of a solid containing needle-like pores ($\alpha = 3$), for three different values of the solid's Poisson's ratio ($\nu = 0.05$; $\nu_0 = 0.25$; $\nu_0 = 0.45$), according to the asymptotic solution (Eq. (62)) (dashed line), and the exact solution (full line).

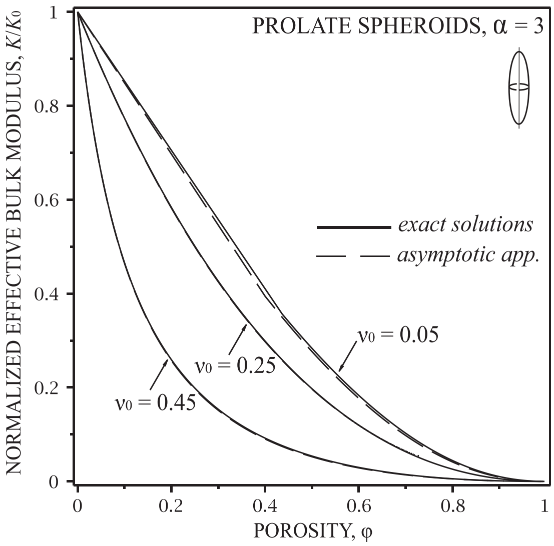

Fig. 5. Normalized effective bulk modulus of a solid containing needle-like pores ($\alpha = 3$), for three different values of the solid's Poisson's ratio ($\nu = 0.05$; $\nu_0 = 0.25$; $\nu_0 = 0.45$), according to the asymptotic solution (combining Eqs. (62) and (63)) (dashed line), and the exact solution (full line).

$$P \sim \frac{3(1-\nu)}{2(1-2\nu)}\left\{1+\frac{4(1+\nu)}{5(7-5\nu)}(1-\alpha)^2\left[1+\frac{83-73\nu}{7(7-5\nu)}(1-\alpha)\right]\right\}, \tag{78}$$

$$Q \sim \frac{15(1-\nu)}{7-5\nu}\left[1+\frac{4(1-\alpha)^2}{175(7-5\nu)^2}\left\{299-7\nu(98-65\nu)+\frac{138079-7\nu[54357-7\nu(7293-2225\nu)]}{49(7-5\nu)}(1-\alpha)\right\}\right]. \tag{79}$$

We now consider $(1-\alpha)$ to be our small parameter, and retain only the quadratic and cubic terms. Extensive calculations lead to the following approximate expressions:

$$\begin{aligned}\ln(1-\phi) = {} & \left[-\frac{1}{6}\ln\left(\frac{1-\nu}{1-\nu_0}\right)+\frac{5}{6}\ln\left(\frac{1-5\nu}{1-5\nu_0}\right)-\frac{2}{3}\ln\left(\frac{1+\nu}{1+\nu_0}\right)\right]+\frac{8}{105}(\alpha-1)^2 \\ & \times\left\{\left(\frac{1}{1-5\nu}-\frac{1}{1-5\nu_0}\right)\left[\frac{2619}{1225}(\alpha-1)-1\right]+\frac{41}{15}\ln\left(\frac{1-5\nu}{1-5\nu_0}\right)\left[\frac{12741}{10045}(\alpha-1)-1\right]\right\},\end{aligned} \tag{80}$$

$$\begin{aligned}\ln\left(\frac{K}{K_0}\right) = {} & \left[\frac{5}{3}\ln\left(\frac{1-5\nu}{1-5\nu_0}\right)-\ln\left(\frac{1-2\nu}{1-2\nu_0}\right)-\frac{2}{3}\ln\left(\frac{1+\nu}{1+\nu_0}\right)\right]+\frac{16}{105}(\alpha-1)^2 \\ & \times\left\{\left(\frac{1}{1-5\nu}-\frac{1}{1-5\nu_0}\right)\left[\frac{2619}{1225}(\alpha-1)-1\right]+\frac{7}{5}\ln\left(\frac{1-5\nu}{1-5\nu_0}\right)\left[\frac{1847}{1715}(\alpha-1)-1\right]\right\}.\end{aligned} \tag{81}$$

The exact solutions (76) and (77) for spherical pores are easily recovered by taking $\alpha = 1$ in expressions (80) and (81).

The expressions (80) and (81) are very accurate in the range $0.7 < \alpha < 1.3$. For example, for $\alpha = 0.7$ and $\phi = 40\%$, the error in both ν and K as a function of the porosity is less than 0.5%, and nearly independent of ν_0 (Figs. 6 and 7).

4. Comparison with the estimates of the Mori–Tanaka and Kuster–Toksoz schemes

We can use the asymptotic expressions for the pores compliances (P, Q) derived by David and Zimmerman (2011) as input in any effective medium theory.

According to the Mori–Tanaka method, and following the previous notations, the effective moduli are described by the following equations (Benveniste, 1987):

$$\frac{K_0}{K(\phi)} = 1+\frac{\phi}{1-\phi}P(\nu_0), \tag{82}$$

$$\frac{G_0}{G(\phi)} = 1+\frac{\phi}{1-\phi}Q(\nu_0). \tag{83}$$

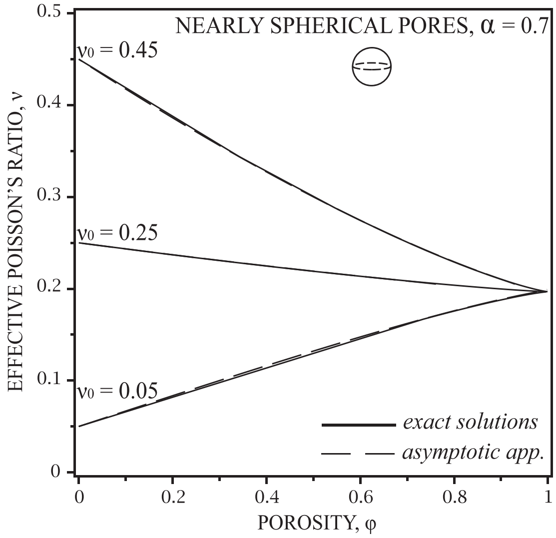

Fig. 6. Effective Poisson's ratio of a solid containing nearly spherical pores ($\alpha = 0.7$), for three different values of the solid's Poisson's ratio ($\nu = 0.05$; $\nu_0 = 0.25$; $\nu_0 = 0.45$), according to the asymptotic solution (Eq. (80)) (dashed line), and the exact solution (full line).

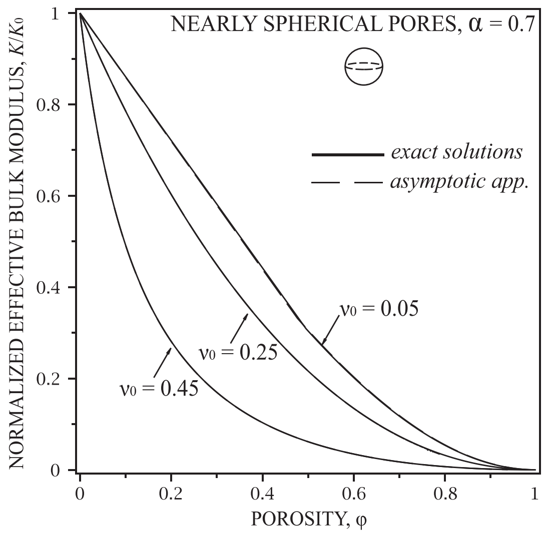

Fig. 7. Normalized effective bulk modulus of a solid containing nearly spherical pores ($\alpha = 0.7$), for three different values of the solid's Poisson's ratio ($\nu = 0.05$; $\nu_0 = 0.25$; $\nu_0 = 0.45$), according to the asymptotic solution (combining Eqs. (80) and (81)) (dashed line), and the exact solution (full line).

If we take the equations for the elastic moduli given by Kuster and Toksoz (1974), and rewrite them in terms of (P, Q) and ν_0, we obtain

$$\frac{K(\phi)}{K_0} = \frac{1 - \phi\frac{2(1-2\nu_0)}{3(1-\nu_0)}P(\nu_0)}{1 + \phi\frac{1+\nu_0}{3(1-\nu_0)}P(\nu_0)}, \tag{84}$$

$$\frac{G(\phi)}{G_0} = \frac{1 - \phi\frac{7-5\nu_0}{15(1-\nu_0)}Q(\nu_0)}{1 + \phi\frac{2(4-5\nu)}{15(1-\nu_0)}Q(\nu_0)}. \tag{85}$$

For the limiting pore geometries, discussions and comparisons of the predictions of the differential, Mori–Tanaka and Kuster and Toksoz theories are numerous in the literature. For example, see Zimmerman (1985, 1991a) for thin cracks, Zimmerman (1991a, 1991b, 1994) for spherical pores; Berryman and Berge (1996) compare the predictions of the Mori–Tanaka and

Kuster–Toksoz theories for needles. Hence, here we will focus only on cases such as crack-like and needle-like pores having finite aspect ratios.

In Figs. 8–13, we compare the predictions of the three effective medium theories for the effective Poisson's ratio and normalized bulk modulus, for the case $\nu_0 = 0.25$, and taking the three values of α that were considered in Section 3: for crack-like pores, $\alpha = 0.3$ (Figs. 8 and 9), for needle-like pores, $\alpha = 3$ (Figs. 10 and 11) and for nearly spherical pores, $\alpha = 0.7$ (Figs. 12 and 13). For the Mori–Tanaka and Kuster–Toksoz theories, the results are obtained by simply inserting the exact or the asymptotic expressions for P and Q into Eqs. (82)–(85), from which calculations of the effective Poisson's ratio are straightforward.

For each three theories, using the simple asymptotic expressions for P and Q rather than the exact expressions introduces errors that are much smaller than are the differences between the predictions of the different theories. Discussion of these errors have already been given for the differential scheme in Section 3. For $\alpha = 0.3$, the errors for the Mori–Tanaka and Kuster–Toksoz estimates of both ν and K are, respectively, 1% and 2% when $\Gamma = 0.31$ ($\phi \sim 30\%$). For $\alpha = 3$ (Figs. 10 and 11), the errors are respectively less than 0.5% and 1% when $\phi = 40\%$. For $\alpha = 0.7$ (Figs. 12 and 13), the errors are approximately 1% and 1.5%. The accuracy obtained when using the asymptotic expressions remains, overall, weakly dependent on ν_0.

5. Behaviour of the effective Poisson's ratio in the high concentration limit

The new asymptotic expressions derived for the differential scheme in Section 3, although they hold for a large range of aspect ratios and porosities, cannot be used to predict the behaviour of the effective Poisson's ratio when the concentration of pores becomes very high. In Fig. 14, we have used the exact solutions for the differential scheme (obtained by numerical integration of Eq. (7)) to show how Poisson's ratio behaves in the high-concentration limit, for different values of α, the spheroid aspect ratio, and ν_0, the solid's Poisson's ratio. The addition of pores drives Poisson's ratio towards a point of attraction ν_c which, for the differential scheme, depends on α but not on ν_0 (Fig. 14). Such behaviour has been noted before by Zimmerman (1994) for spherical pores, and by Berryman et al. (2002) for oblate spheroids and needles.

The value ν_c is a *fixed-point* for the Poisson's ratio, which by definition satisfies $F_\nu(\nu_c) = d\nu/d\phi = 0$ in Eq. (7). The right-hand side of Eq. (7) shoes that ν_c is a fixed-point if, for a given α, either $P(\nu_c) = Q(\nu_c)$, $\nu_c = -1$, or $\nu_c = 0.5$. Although it is difficult to prove by analytical methods, numerical simulations show that for any fixed value of α, the pore compressibility P and the shear compliance Q are respectively increasing and decreasing functions of ν. Furthermore, when $\nu = 0$, P is always lower than Q. Hence, a point of intersection between P and Q always exists somewhere between $\nu = 0$ and $\nu = 0.5$, and is unique. Moreover, this point corresponds to an *attractor*: when $0 < \nu < \nu_c$, $P < Q$ and hence $F_\nu > 0$; whereas when $\nu_c < \nu < 0.5$, $P > Q$ and hence $F_\nu < 0$. Following the same argument, the other possible fixed-point that lies within the physically meaningful range, $\nu_c = 0.5$, is an unstable point. This is proven by noting that, because ν_c never exceeds a value approximately equal to 0.2 (see Fig. 15), and $F_\nu < 0$ when $\nu > \nu_c$, small deviations from the value 0.5 cause the effective Poisson's ratio to decrease. As a result, the attraction point for the Poisson's ratio, ν_c, is unique and is implicitly defined, for a given value of α, by:

$$P(\nu_c) = Q(\nu_c). \tag{86}$$

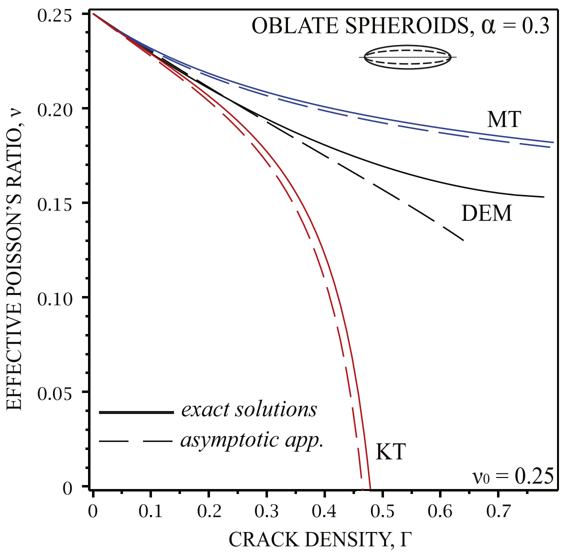

Fig. 8. Effective Poisson's ratio of a solid containing crack-like pores of aspect ratio $\alpha = 0.3$, according to the differential, Mori–Tanaka and Kuster and Toksoz schemes. For each of the three effective medium theories, the solid line represents the exact solution, and the dashed line represents the asymptotic expression. The Poisson's ratio of the solid is $\nu_0 = 0.25$.

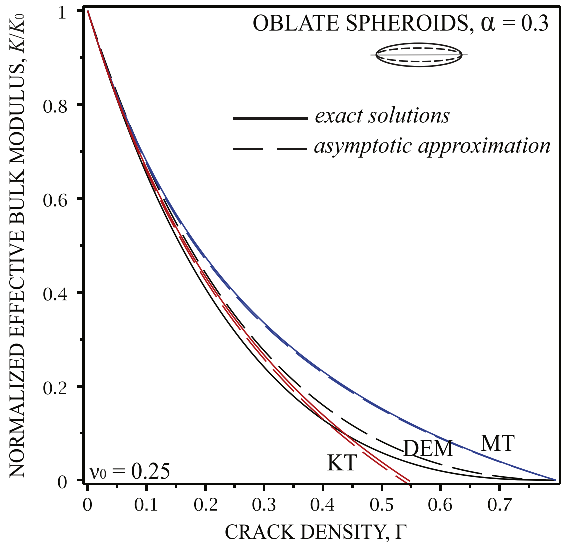

Fig. 9. Normalized effective bulk modulus of a solid containing crack-like pores of aspect ratio $\alpha = 0.3$, according to the differential, Mori–Tanaka and Kuster and Toksoz schemes. For each of the three effective medium theories, the solid line represents the exact solution, and the dashed line represents the asymptotic expression. The Poisson's ratio of the solid is $\nu_0 = 0.25$.

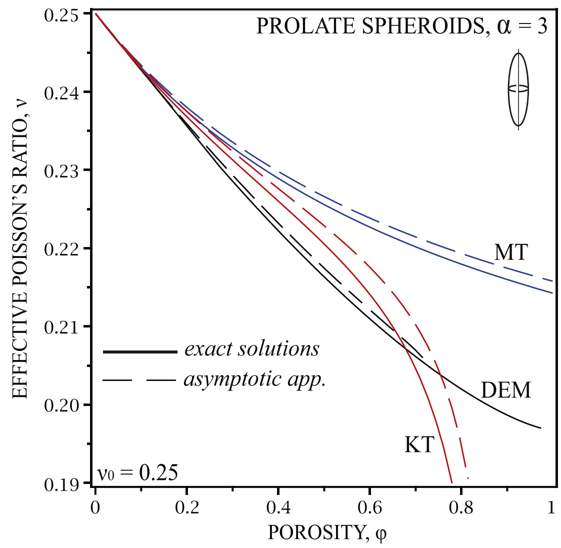

Fig. 10. Effective Poisson's ratio of a solid containing needle-like pores of aspect ratio $\alpha = 3$, according to the differential, Mori–Tanaka and Kuster and Toksoz schemes. For each of the three effective medium theories, the solid line represents the exact solution, and the dashed line represents the asymptotic expression. The Poisson's ratio of the solid is $\nu_0 = 0.25$.

For the limiting geometries (flat cracks, spheres, needles), the fixed-point can found directly by solving the equation $P = Q$. For thin cracks, we find $\nu_c = 0$; for spheres, $\nu_c = 0.2$; and for infinitely long needles, $\nu_c = \lambda = (7 - \sqrt{29})/8 \approx 0.202$, thus recovering the results of Zimmerman (1991b) for spheres, and Berryman et al. (2002) for thin cracks and needles.

The fixed-point ν_c varies rapidly with α when the pores are crack-like (Fig. 15). On the other hand, for prolate spheroids the fixed-point is almost insensitive to α, and is close to the value obtained for spheres ($\nu_c = 0.2$). Indeed, the maximum of ν_c, found for infinitely long needles, is $\nu_c \approx 0.202$. Note that apart from the limiting cases, the values of ν_c must be found numerically. However, the following approximation is quite accurate for the entire range of aspect ratios (Fig. 15):

$$\nu_c = 0.2(1 - e^{-5\alpha}). \tag{87}$$

Because Poisson's ratio is bounded between the fixed point, ν_c and the solid's Poisson's ratio, ν_0, considerable information on the microstructure can be simply inferred from measurements of Poisson's ratio in a porous rock. Consider the example of a porous rock, whose solid's Poisson's ratio is equal to 0.25, compressed to a pressure sufficiently high that we can assume that

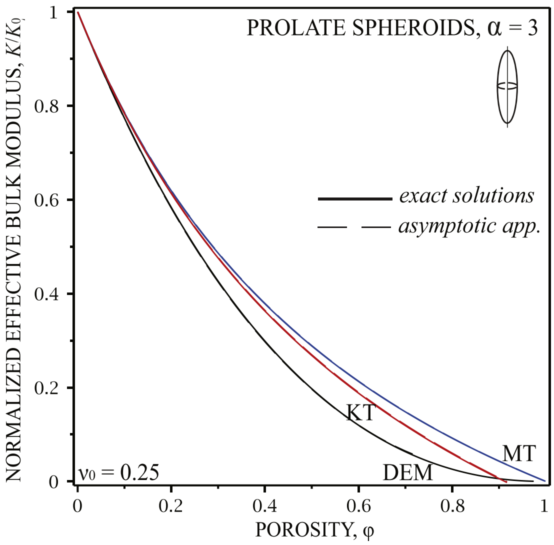

Fig. 11. Normalized effective bulk modulus of a solid containing needle-like pores of aspect ratio $\alpha = 3$, according to the differential, Mori–Tanaka and Kuster and Toksoz schemes. For each of the three effective medium theories, the solid line represents the exact solution, and the dashed line represents the asymptotic expression. The Poisson's ratio of the solid is $\nu_0 = 0.25$.

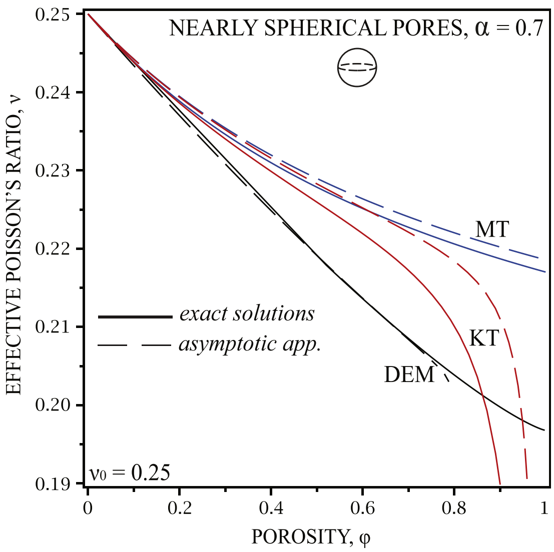

Fig. 12. Effective Poisson's ratio of a solid containing nearly spherical pores of aspect ratio $\alpha = 0.7$, according to the differential (red), Mori–Tanaka (blue) and Kuster and Toksoz (black) schemes. For each of the three effective medium theories, the solid line represents the exact solution, and the dashed line represents the asymptotic expression. The Poisson's ratio of the solid is $\nu_0 = 0.25$. (For interpretation of the references to colour in this figure legend, the reader is referred to the web version of this article.)

all the compliant cracks are closed. Assume for simplicity that all the pores have more or less the same aspect ratio. If the Poisson's ratio of the solid material is 0.25, and the effective Poisson's ratio of the porous rock is 0.15, we can infer from Eq. (87) that the mean aspect ratio of the non-closable porosity must not exceed the value $-0.2 \times \ln(1 - 5 \times 0.15) \approx 0.3$. In other words, pore aspect ratios higher that 0.3 cannot explain a value of ν as low as 0.15.

The Kuster and Toksoz scheme fails to predict realistic behaviour of Poisson's ratio at high porosities, since for any value of α, the predicted values of ν become negative at porosities lower than 100%; see, for instance, Figs. 8, 10 and 12. Hence, discussion of the behaviour of ν for high porosities is not so meaningful for this theory. On the other hand, such a study is of interest with regards to the Mori–Tanaka model. In fact, an extensive study of the fixed-points for the Mori–Tanaka scheme has been done by Dunn and Ledbetter (1995), for the entire range of aspect ratios. To find the fixed-point, Dunn and Ledbetter (1995) started from the equation giving ν as a function of ν_0 and ϕ, for a given α, which can easily be found combining Eqs. (82) and (83):

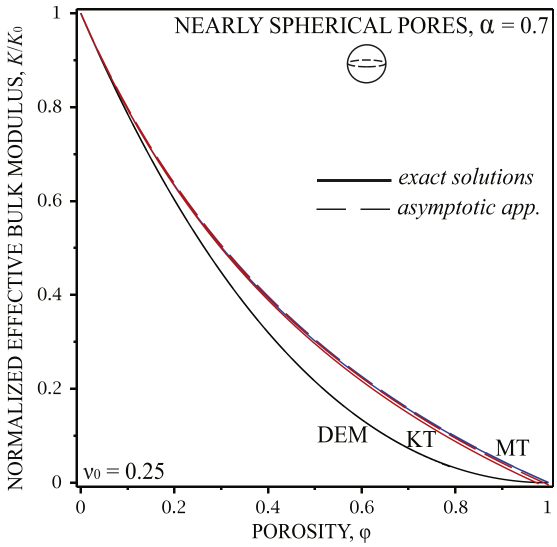

Fig. 13. Normalized effective bulk modulus of a solid containing nearly spherical pores of aspect ratio $\alpha = 0.7$, according to the differential (red), Mori–Tanaka (blue) and Kuster and Toksoz (black) schemes. For each of the three effective medium theories, the solid line represents the exact solution, and the dashed line represents the asymptotic expression. The Poisson's ratio of the solid is $v_0 = 0.25$. (For interpretation of the references to colour in this figure legend, the reader is referred to the web version of this article.)

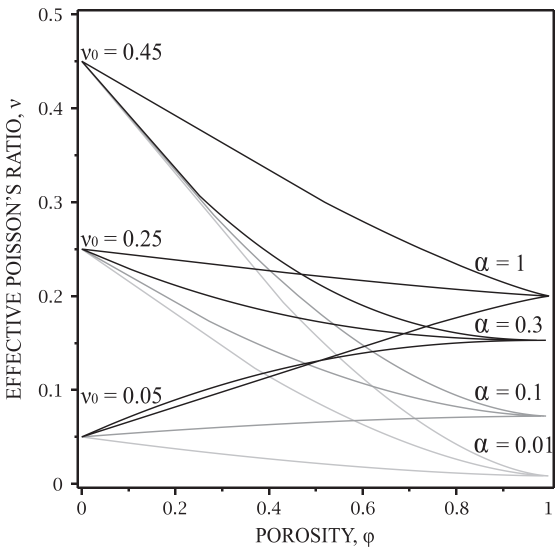

Fig. 14. Effective Poisson's ratio as a function of the porosity, for various values of the inclusion aspect ratio ($\alpha = 0.01$; $\alpha = 0.1$; $\alpha = 0.3$; $\alpha = 1$) and the solid's Poisson's ratio ($v_0 = 0.05$; $v_0 = 0.25$; $v_0 = 0.45$), according to the differential scheme. For $\alpha = 0.01$, $\alpha = 0.1$, $\alpha = 0.3$, the solutions were found by numerical integration of Eq. (7); for spherical pores, from Eq. (76).

$$v = \frac{3v_0(1-\phi) + \phi[(1+v_0)Q(v_0) - (1-2v_0)P(v_0)]}{3(1-\phi) + \phi[2(1+v_0)Q(v_0) + (1-2v_0)P(v_0)]}. \tag{88}$$

They set $v = v_0$ and solved for v_0 to obtain the fixed-point, which they defined as that particular value of the solid-phase Poisson's ratio that would not be changed by the addition of pores. However, they did not seem to have gone as far as noticing that the fixed-point they found for the Mori–Tanaka scheme also satisfies the condition $P(v_0) = Q(v_0)$. Indeed, if we insert this conditions in Eq. (88), we find

$$v = \frac{3v_0(1-\phi) + 3v_0\phi P(v_0)}{3(1-\phi) + 3\phi P(v_0)} = v_0, \tag{89}$$

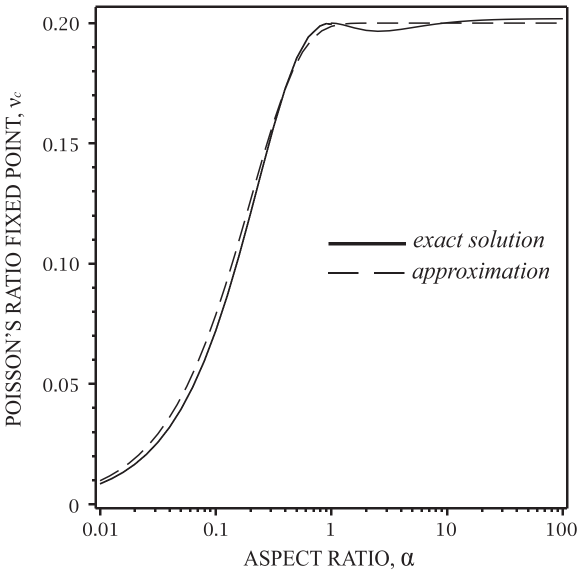

Fig. 15. Fixed-point for the Poisson's ratio, ν_c, solution of Eq. (86), as a function of the inclusion aspect ratio, α (full-line); the approximation (87) is also shown (dashed line).

which shows that, according to the differential and Mori–Tanaka schemes, all considerations on the fixed-point of Poisson's ratio are totally equivalent. However, whereas the differential scheme predicts that the effective Poisson's ratio approaches the fixed point as the porosity approaches 1, according to the Mori–Tanaka scheme the effective Poisson ratio tends towards ν_c, but does not reach this value when $\phi = 1$. This is discussed for the special case of spheres by Zimmerman (1991b).

6. Conclusion

The asymptotic expressions for the pore compliances P and Q recently derived by David and Zimmerman (2011) for (P, Q) have been used as input in the differential scheme, as well as the Mori–Tanaka and Kuster–Toksoz theories, to obtain approximate analytical solutions for the effective moduli. The equations of the differential scheme have been integrated to yield expressions that hold for a wide range of aspect ratios and porosities, yet remain simple. Using these expressions would considerably simplify the process of inverting sonic velocity data to obtain pore aspect ratio distributions (in rocks, for instance, see Hadley (1976), Cheng & Toksoz (1979)). Finally, a discussion was given of the effective Poisson ratio, which tends towards a fixed point ν_c that depends only on the pore aspect ratio, but not on the Poisson's ratio of the solid phase, ν_0. The fact that Poisson's ratio is bounded by these two values allows a rapid estimation of pore shape to be inferred from the effective Poisson's ratio, as shown by our simple example discussed above.

References

Benveniste, Y. (1987). A new approach to the application of Mori–Tanaka's theory in composite materials. *Mechanics of Materials, 6*, 147–157.

Berryman, J. G., & Berge, P. A. (1996). Critique of explicit schemes for estimating elastic properties of multiphase composites. *Mechanics of Materials, 22*, 149–164.

Berryman, J. G., Pride, S. R., & Wang, H. F. (2002). A differential scheme for elastic properties of rocks with dry or saturated cracks. *Geophysical Journal International, 151*, 597–611.

Bruner, W. M. (1976). Comment on "Seismic velocities in dry and cracked solids" by Richard J. O'Connell and Bernard Budiansky. *Journal of Geophysical Research, 81*, 2573–2576.

Carvalho, F. C. S., & Labuz, J. F. (1996). Experiments on effective elastic modulus of two-dimensional solids with cracks and holes. *International Journal of Solids and Structures, 33*, 4119–4130.

Cheng, C. H., & Toksoz, M. N. (1979). Inversion of seismic velocities for the pore aspect ratio spectrum of a rock. *Journal of Geophysical Research, 84*, 7533–7543.

David, E. C., & Zimmerman, R. W. (2011). Compressibility and shear compliance of spheroidal pores: Exact derivation via the Eshelby tensor, and asymptotic expressions in limiting cases. *International Journal of Solids and Structures, 48*, 680–688.

Dunn, M. L., & Ledbetter, H. (1995). Poisson's ratio of porous and microcracked solids: Theory and application to oxyde superconductors. *Journal of Materials Research, 10*, 2715–2722.

Eshelby, J. D. (1957). The determination of the elastic field of an ellipsoidal inclusion, and related problems. *Proceedings of the Royal Society of London A, 241*, 376–396.

Hadley, K. (1976). Comparison of calculated and observed cracked densities and seismic velocities in Westerly granite. *Journal of Geophysical Research, 81*, 3484–3494.

Hashin, Z., & Shtrikman, S. (1961). Note on a variational approach to the theory of composite elastic materials. *Journal of The Franklin Institute, 271*, 336–341.

Henyey, F. S., & Pomphrey, N. (1982). Self-consistent elastic moduli of a cracked solid. *Geophysical Research Letters, 9*, 903–906.

Kuster, G. T., & Toksoz, M. N. (1974). Velocity and attenuation of seismic waves in two-phase media: Part I. Theoretical formulations. *Geophysics, 39*, 587–606.

LeRavalec, M., & Gueguen, Y. (1996). High- and low-frequency elastic moduli for a saturated porous/cracked rock – Differential self-consistent and poroelastic theories. *Geophysics, 61*, 1080–1094.

McLaughlin, R. (1977). A study of the differential scheme for composite materials. *International Journal of Engineering Science, 15*, 237–244.

Mori, T., & Tanaka, K. (1973). Average stress in matric and average elastic energy of materials with misfitting inclusions. *Acta Materialia, 21*, 571–574.

Norris, A. N. (1985). A differential scheme for the effective moduli of composites. *Mechanics of Materials, 4*, 1–16.

Saenger, E. H., Kruger, O. S., & Shapiro, S. A. (2004). Effective elastic properties of randomly fractured soils: 3D numerical experiments. *Geophysical Prospecting, 52*, 183–195.

Saenger, E. H., Kruger, O. S., & Shapiro, S. A. (2006). Effective elastic properties of fractured rocks: Dynamic vs. static considerations. *International Journal of Fracture, 139*, 569–576.

Salganik, R. L. (1973). Mechanics of bodies with many cracks. *Mechanics of Solids, 8*, 135–143.

Shen, L., & Li, J. (2004). A numerical simulation for effective elastic moduli of plates with various distributions and sizes of cracks. *International Journal of Solids Structures, 41*, 7471–7492.

Walsh, J. B. (1965). The effect of cracks on the compressibility of rocks. *Journal of Geophysical Research, 70*, 381–389.

Wilkens, R., Simmons, G., & Caruso, L. (1984). The ratio V_p/V_s as a discriminant of composition for siliceous sandstones. *Geophysics, 49*, 1850–1860.

Zimmerman, R. W. (1984). Elastic moduli of a solid with spherical pores: New self-consistent method. *International Journal of Rock Mechanics and Mining Sciences, 21*, 339–343.

Zimmerman, R. W. (1985). The effect of microcracks on the elastic moduli of brittle materials. *Journal of Materials Science Letters, 4*, 1457–1460.

Zimmerman, R. W. (1991a). *Compressibility of sandstones*. Amsterdam: Elsevier.

Zimmerman, R. W. (1991b). Elastic moduli of a solid containing spherical inclusions. *Mechanics of Materials, 12*, 17–24.

Zimmerman, R. W. (1994). Behaviour of the Poisson ratio of a two-phase composite material in the high-concentration limit. *Applied Mechanics Reviews, 47*, 38–43.